Metabolic Engineering 13 (2011) 733–744

Contents lists available at SciVerse ScienceDirect

Metabolic Engineering

journal homepage: www.elsevier.com/locate/ymben

Identification of bottlenecks in *Escherichia coli* engineered for the production of CoQ_{10}

Corinne P. Cluis [a,1], Andrew Ekins [a,1], Lauren Narcross [a], Heng Jiang [a], Nicholas D. Gold [a], Adam M. Burja [b,2], Vincent J.J. Martin [a,*]

[a] Department of Biology, Concordia University, 7141 Sherbrooke West, Montréal, Québec, Canada H4B 1R6
[b] Ocean Nutrition Canada, Fermentation and Metabolic Engineering Group, 101 Research Drive, Dartmouth, Nova Scotia, Canada B2Y 4T6

ARTICLE INFO

Article history:
Received 4 July 2011
Received in revised form
7 September 2011
Accepted 26 September 2011
Available online 4 October 2011

Keywords:
Coenzyme Q_{10}
Ubiquinone
Decaprenyl diphosphate synthase
Escherichia coli
Metabolic engineering

ABSTRACT

In this work, *Escherichia coli* was engineered to produce a medically valuable cofactor, coenzyme Q_{10} (CoQ_{10}), by removing the endogenous octaprenyl diphosphate synthase gene and functionally replacing it with a decaprenyl diphosphate synthase gene from *Sphingomonas baekryungensis*. In addition, by over-expressing genes coding for rate-limiting enzymes of the aromatic pathway, biosynthesis of the CoQ_{10} precursor *para*-hydroxybenzoate (PHB) was increased. The production of isoprenoid precursors of CoQ_{10} was also improved by the heterologous expression of a synthetic mevalonate operon, which permits the conversion of exogenously supplied mevalonate to farnesyl diphosphate. The over-expression of these precursors in the CoQ_{10}-producing *E. coli* strain resulted in an increase in CoQ_{10} content, as well as in the accumulation of an intermediate of the ubiquinone pathway, decaprenylphenol (10P-Ph). In addition, the over-expression of a PHB decaprenyl transferase (UbiA) encoded by a gene from *Erythrobacter* sp. NAP1 was introduced to direct the flux of DPP and PHB towards the ubiquinone pathway. This further increased CoQ_{10} content in engineered *E. coli*, but decreased the accumulation of 10P-Ph. Finally, we report that the combined over-production of isoprenoid precursors and over-expression of UbiA results in the decaprenylation of *para*-aminobenzoate, a biosynthetic precursor of folate, which is structurally similar to PHB.

1. Introduction

Coenzyme Q_n (CoQ_n), otherwise known as ubiquinone, is a redox-active biomolecule formed by the conjugation of a benzoquinone head group to an isoprenoid chain of varying length. The number (n) of isoprene units forming the lipid chain of CoQ_n varies between species: humans mainly synthesize CoQ harboring a ten-unit *E*-isoprenoid (CoQ_{10}), while *Saccharomyces cerevisiae* produces CoQ_6 and *Escherichia coli*, CoQ_8. In bacteria, CoQ_n is embedded in the cytoplasmic membrane where it acts as an electron carrier in the respiratory chain and plays a role in the formation of disulfide bonds (Bader et al., 2000; Ingledew and Poole, 1984). While CoQ_n typically takes part in prokaryotic aerobic respiration, other quinones, such as menaquinone (MK_n), are active during anaerobic respiration (Ingledew and Poole, 1984; Wissenbach et al., 1990). In eukaryotes, CoQ_n participates in the electron transport chain by transferring electrons between the different respiratory complexes and additionally acts as a cofactor for the mitochondrial uncoupling protein, within the mitochondrial inner membrane (Echtay et al., 2000; Kroger and Klingenberg, 1973). Also present in other organelles, CoQ_n plays an additional role as an antioxidant by protecting membrane lipids and proteins from oxidation, either by scavenging free radicals directly or by regenerating the pool of tocopherol (Lass and Sohal, 1998; Martin et al., 2007; Yoshida et al., 2006). Moreover, CoQ_n is involved in the regulation of several genes, some of which play roles in cholesterol metabolism and in inflammatory responses (Schmelzer et al., 2007, 2010).

The benefits of CoQ_{10} supplementation to patients with cardiovascular diseases, including conjunctive heart failure and acute myocardial infarction, as well as certain neurodegenerative diseases and diabetes have been documented (Hodgson et al., 2002; Shults et al., 2002; Singh et al., 1998; Yang et al., 2010). Besides these clinical benefits, the topical application of CoQ_{10} was shown to reduce wrinkle formation, resulting in its incorporation in a number of cosmetic dermatology formulations (Inui et al., 2008).

Because of the growing demand from the pharmaceutical and cosmetic industries, research into the development of a bioprocess leading to the commercial production of CoQ_{10} has intensified.

Abbreviations: CoQ_{10}, coenzyme Q_{10}; DPP, decaprenyl diphosphate; DPS, decaprenyl diphosphate synthase; PABA, *para*-aminobenzoate; PHB, *para*-hydroxybenzoate; 10P-AB, 3-decaprenyl-4-aminobenzoate; 10P-HB, 3-decaprenyl-4-hydroxybenzoate; 10P-Ph, decaprenylphenol; SA, shikimic acid

* Corresponding author. Fax: +1 514 848 4504.
E-mail address: vmartin@alcor.concordia.ca (V.J.J. Martin).

[1] These authors contributed equally.

[2] Current address: BP Biofuels, BP Alternative Energy International Ltd., Global Technology Centre, 4955 Directors Place, San Diego, CA, USA.

1096-7176/$ - see front matter © 2011 Elsevier Inc. All rights reserved.
doi:10.1016/j.ymben.2011.09.009

With the aim of developing a microbial production platform, several groups have studied natural producers of CoQ_{10}, including *Agrobacterium tumefaciens* and *Rhodobacter sphaeroides*. Improvements in cell titers and yields of CoQ_{10} using such microbes have been obtained using chemical mutagenesis and the optimization of fermentation conditions (Choi et al., 2005; Gu et al., 2006; Ha et al.,

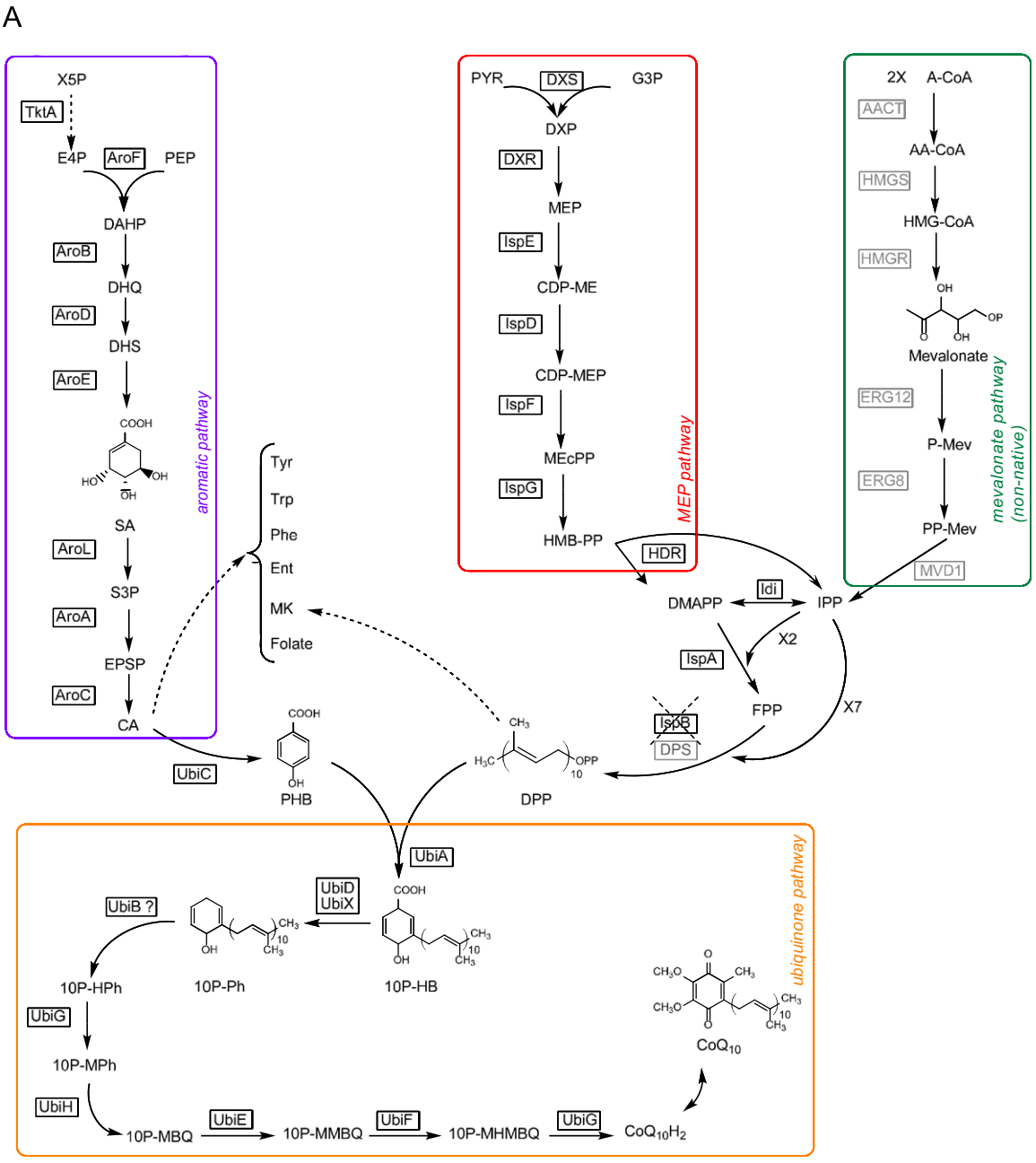

2007a, 2007b; Kien et al., 2010; Sakato et al., 1992; Wu et al., 2003; Yen et al., 2010; Yen and Shih, 2009).

Although *E. coli* naturally synthesizes CoQ_8 rather than CoQ_{10}, its robust fermentation characteristics and amenability to genetic modifications provide great potential for industrial applications. Moreover, the biochemical pathway leading to the biosynthesis of CoQ_n in *E. coli* has been almost entirely deciphered (Fig. 1A), resulting in its use as a host for CoQ_{10} production. The biosynthesis of CoQ_{10} by *E. coli* is made possible by the expression of an *E*-decaprenyl diphosphate (DPP) synthase (DPS), along with the optional deletion of *ispB*, coding for *E*-octaprenyl diphosphate synthase, in order to eliminate the synthesis of CoQ_8 (Fig. 1A) (Choi et al., 2009; Kim et al., 2006; Lee et al., 2004; Okada et al., 1998; Park et al., 2005; Takahashi et al., 2003; Zahiri et al., 2006a, 2006b). Knowledge of the biochemical pathway and genes involved in CoQ_n biosynthesis has led to the development of rational genetic engineering strategies to improve yields of CoQ_{10} in *E. coli*. For instance, improvements in CoQ_{10} titers have been made by over-expressing 1-deoxy-D-xylulose 5-phosphate synthase (DXS) of the methylerythritol phosphate pathway (MEP) with the goal of increasing the availability of isopentenyl diphosphate (IPP) and dimethylallyl diphosphate (DMAPP) (Fig. 1A) (Choi et al., 2009; Harker and Bramley, 1999; Kim et al., 2006). Additionally, a foreign mevalonate pathway was expressed in *E. coli*, resulting in higher CoQ_{10} content (Zahiri et al., 2006b). The effect of the augmented production of isoprenoids is potentiated by an exogenous supply of the aromatic precursor to CoQ_n, *para*-hydroxybenzoate (PHB), suggesting that both isoprenoid and aromatic metabolites are limiting CoQ_n production in *E. coli* (Zahiri et al., 2006b). Accordingly, the over-expression of UbiC, which converts chorismate into PHB (Fig. 1A), also results in an increase in CoQ_n production (Zhang et al., 2007; Zhu et al., 1995). However, no attempt has been made to improve PHB production by deregulating and over-expressing the aromatic pathway of *E. coli*. Downstream of these primary metabolic pathways, the aromatic and isoprenoid moieties of CoQ_{10} are condensed into a single molecule and further modified by a series of ring modifications, via the ubiquinone pathway (Fig. 1A). Studies aimed at assessing the impact of the over-expression of selected enzymes of this pathway suggest that UbiA is rate limiting, while the over-expression of UbiB, UbiG and UbiH has little impact on CoQ_n production (Zhang et al., 2007; Zhu et al., 1995). Nevertheless, these genes were over-expressed in *E. coli* strains where the production of isoprenoid and aromatic precursors were endogenously regulated and thus, were potentially limiting. Therefore, it is possible that the modest increases in CoQ_n content reported in these studies are a result of the limited carbon flux to the ubiquinone pathway. Overall, despite its great potential as a production host, the CoQ_{10} content currently obtained in engineered *E. coli* (2.5 mg/g dry cell weight (DCW)) still falls below those obtained in mutant strains of *A. tumefaciens* (11.84 mg/g DCW) and *R. sphaeroides* (8.7 mg/g DCW) (Ha et al., 2009; Yoshida et al., 1998; Zahiri et al., 2006b).

In this research, we sought to bypass endogenous restrictions in carbon flux towards the ubiquinone pathway in a CoQ_{10}-producing *E. coli* strain by expressing a DPS from a marine bacterium. To do so, we engineered the production of augmented concentrations of both the aromatic precursor, PHB, and the isoprenoid intermediates, IPP and FPP. Moreover, in order to further channel these precursors towards CoQ_{10} production, we over-expressed a PHB decaprenyl transferase (UbiA) derived from a CoQ_{10}-producing bacterium. Using this approach, we sought to gain new insights into the control of CoQ_{10} biosynthesis in the context of an *E. coli* production platform, and to identify bottlenecks limiting the accumulation of CoQ_{10} in this host. We report that the deregulated over-production of both aromatic and isoprenoid precursors of CoQ_{10} results in the accumulation of decaprenylphenol, and that the production of this intermediate is modulated by the expression of UbiA. We also report that the over-expression of UbiA coupled with higher isoprenoid biosynthesis, yet uncoupled to a corresponding increase in PHB production, results in the accumulation of decaprenyl-aminobenzoate. We hypothesize that the accumulation of this compound results from the prenylation of *para*-aminobenzoate by UbiA.

2. Methods

2.1. Reagents, strains and culture conditions

E. coli strains and plasmids used in this study are listed in Table 1. *E. coli* DH5α was used for cloning whereas CoQ_{10}-producing strains were constructed in *E. coli* MG1655. *E. coli* strains containing the individual gene knockouts Δ*aroK*::*kan*, Δ*aroL*::*kan*, Δ*aroA*::*kan* and Δ*aroC*::*kan* were obtained from the Keio collection (Baba et al., 2006). Multiple gene knockouts and insertions in *E. coli* MG1655 were generated by P1 transduction as previously described (Thomason et al., 2007). When required, strains were propagated on LB media supplemented with 100 μg/mL ampicillin, 20 μg/mL chloramphenicol, 12.5 μg/mL tetracycline and/or 25 μg/mL kanamycin. Polymerase chain reactions (PCR) for cloning purposes were performed with Phusion High-Fidelity DNA polymerase (New England Biolabs) while colony PCR reactions to identify positive clones were conducted using *Taq* DNA polymerase (Fermentas). DNA isolated from agarose gels and PCR reactions were purified using the QIAquick Gel and QIAquick PCR purification kit (Qiagen), respectively. Plasmid extractions were done using the GeneJET Plasmid Miniprep Kit (Fermentas). Chemicals were obtained from Sigma-Aldrich. Mevalonate was prepared from D,L-mevalolactone as previously described (Martin

Fig. 1. Engineering *E. coli* for CoQ_{10} production. (A) Biosynthetic pathway leading to the formation of CoQ_{10} in *E. coli*. Enzymes in black are endogenous to *E. coli*. Enzymes in gray are non-native to *E. coli*. Pathway intermediates: X5P, D-xylulose-5-phosphate; E4P, D-erythrose-4-phosphate; PEP, phosphoenolpyruvate; DAHP, 3-deoxy-arabino-heptulosonate 7-phosphate; DHQ, 3-dehydroquinate; DHS, 3-dehydroshikimate; SA, shikimic acid; S3P, shikimate-3-phosphate; EPSP, 5-enolpyruvyl-shikimate-3-phosphate; CA, chorismic acid; Tyr, L-tyrosine; Trp, L-tryptophan; Phe, L-phenylalanine; Ent, enterobactin; MK, menaquinone; PHB, *para*-hydroxybenzoate; PYR, pyruvate; G3P, D-glyceraldehyde-3-phosphate; DXP, 1-deoxy-D-xylulose-5-phosphate; MEP, 2-C-methyl-D-erythrithol-5-phosphate; CDP-ME, 4-diphosphocytidyl-2C-methyl-D-erythritol; CDP-MEP, 4-diphosphocytidyl-2C-methyl-D-erythritol 2-phosphate; MEcPP, 2-C-methyl-D-erythritol-2,4-cyclodiphosphate; 'HMB-PP, 1-hydroxy-2-methyl-2-(E)-butenyl 4-diphosphate; A-CoA, acetylcoenzyme-A; AA-CoA, acetoacetylcoenzyme-A; HMG-CoA, 3-hydroxy-3-methylglutaryl-coenzyme-A; mevalonate, *R*-mevalonate; P-Mev, mevalonate-5-phosphate; PP-Mev, mevalonate-diphosphate; DMAPP, dimethylallyl diphosphate; IPP, isopentenyl diphosphate; FPP, (*E,E*)-farnesyl diphosphate; DPP, *E*-decaprenyl diphosphate; 10P-HB, 3-decaprenyl-4-hydroxybenzoate; 10P-Ph, 2-decaprenylphenol; 10P-HPh, 2-decaprenyl-6-hydroxyphenol; 10P-MPh, 2-decaprenyl-6-methoxyphenol; 10P-MBQ, 2-decaprenyl-6-methoxy-1,4-benzoquinol; 10P-MMBQ, 2-decaprenyl-3-methyl-6-methoxy-1,4-benzoquinol; 10-MHMBQ, 2-decaprenyl-3-methyl-5-hydroxy-6-methoxy-1,4-benzoquinol; $CoQ_{10}H_2$, ubiquinol-10; CoQ_{10}, coenzyme Q_{10}. (B) Synthetic operons used in this study. $pTDPS_o$, derived from the plasmid pTrc99A, contains dps_o, coding for a decaprenyl diphosphate synthase, and driven by the *trc* promoter. $pTUbiA_oDPS_o$, derived from the plasmid pTrc99A, contains $ubiA_o$, coding for a PHB decaprenyl transferase, and dps_o, driven by the *trc* promoter. pALTAA, derived from the plasmid pAlac, contains *tktA*, coding for a transketolase, $aroF^{FBR}$, coding for a tyrosine-insensitive 3-deoxy-D-arabino-heptulosonate 7-phosphate synthase and *aroB*, coding for a 3-dehydroquinate synthase, driven by P_{lacZ}. *ubiC*::LLACC contains *aroL*, coding for a shikimate kinase, *aroA*, coding for a 5-enolpyruvyl-shikimate-3-phosphate synthase, *aroC*, coding for a chorismate synthase and *ubiC*, coding for a chorismate lyase, driven by P_{lacZ} and integrated downstream of *ubiC* on the chromosome. pMBIS, derived from the plasmid pBBR1MCS3, contains *ERG12*, coding for a mevalonate kinase, *ERG8*, coding for a phosphomevalonate kinase, *MVD1*, coding for a mevalonate pyrophosphate decarboxylase, *idi*, coding for an IPP isomerase and *ispA*, coding for a FPP synthase, driven by P_{lacZ}.

Table 1
Strains and plasmids used in this study.

Strain	Genotype/description	Reference
DH5α	*fhuA2 Δ(argF-lacZ)U169 phoA glnV44 Φ80 Δ(lacZ)M15 gyrA96 recA1 relA1 endA1 thi-1 hsdR17*	Invitrogen
BW25113	$rrnB_{T14}$ $\Delta lacZ_{WJ16}$ *hsdR*514 $\Delta araBAD_{AH33}$ $\Delta rhaBAD_{LD78}$	Datsenko and Wanner (2000)
MG1655	F-λ-*ilvG-rfb*-50 *rph*-1	ATCC 700926
CC1.D	MG1655 + $pTDPS_o$	This study
CC2.D	MG1655, Δ*ispB* + $pTDPS_o$	This study
CC1.1	MG1655 + pALac	This study
CC1.1.ARO1	MG1655 + pALTAA	This study
CC3.1	MG1655, Δ*aroK*, Δ*aroL* + pALac	This study
CC3.1.ARO1	MG1655, Δ*aroK*, Δ*aroL* + pALTAA	This study
CC1.1.ARO2	MG1655, *ubiC*::*LLACC* + pALac	This study
CC1.1.ARO3	MG1655, *ubiC*::*LLACC* + pALTAA	This study
CC2.D.1	MG1655, Δ*ispB* + $pTDPS_o$ + pALac + pBBR1MCS3	This study
CC2.D.1.ISO1	MG1655, Δ*ispB* + $pTDPS_o$ + pALac + pMBIS	This study
CC2.D.1.ARO3	MG1655, Δ*ispB*, *ubiC*::*LLACC* + $pTDPS_o$ + pALTAA + pBBR1MCS3	This study
CC2.D.1.ARO3.ISO1	MG1655, Δ*ispB*, *ubiC*::*LLACC* + $pTDPS_o$ + pALTAA + pMBIS	This study
CC2.DU.1	MG1655, Δ*ispB* + $pTUbiA_oDPS_o$ + pALac + pBBR1MCS3	This study
CC2.DU.1.ISO1	MG1655, Δ*ispB* + $pTUbiA_oDPS_o$ + pALac + pMBIS	This study
CC2.DU.1.ARO3	MG1655, Δ*ispB*, *ubiC*::*LLACC* + $pTUbiA_oDPS_o$ + pALTAA + pBBR1MCS3	This study
CC2.DU.1.ARO3.ISO1	MG1655, Δ*ispB*, *ubiC*::*LLACC* + $pTUbiA_oDPS_o$ + pALTAA + pMBIS	This study
Plasmid	**Description**	**Reference**
pACYC184	Low-copy expression plasmid; Tet^R, Cm^R	ATCC 37033
pALac	pACYC184 derivative containing the *lacZ* promoter; Cm^R	This study
$pALDPS_o$	pALac derivative containing DPS_o; Cm^R	This study
pTrc99A	High-copy expression plasmid; Amp^R	Pharmacia
$pTDPS_o$	pTrc99A derivative containing DPS_o; Amp^R	This study
$pTUbiA_oDPS_o$	pTrc99A derivative containing $ubiA_o$ and DPS_o; Amp^R	This study
pKD4	Plasmid with the RK6γ origin containing a Kan^R cassette flanked by FRT sites; Amp^R	Datsenko and Wanner (2000)
pKD46	Plasmid with repA101(ts) origin containing *araBp-gam-bet-exo* for λ red recombination; Amp^R	Datsenko and Wanner (2000)
pCP20	Plasmid with temperature sensitive origin of replication containing the *FLP*; Amp^R, Cm^R	Datsenko and Wanner (2000)
pGEM-T Easy	High-copy cloning plasmid; Amp^R	Promega
pG-TktA	pGEM-T Easy derivative containing *tktA*; Amp^R	This study
pG-AroF	pGEM-T Easy derivative containing *aroF*; Amp^R	This study
pG-AroFFBR	pGEM-T Easy derivative containing $aroF^{FBR}$; Amp^R	This study
pG-AroB	pGEM-T Easy derivative containing *aroB*; Amp^R	This study
pGFPuv	High-copy plasmid containing P_{lacZ}-*GFPuv*; Amp^R	ClonTech
pUC19	High-copy cloning plasmid; Amp^R	Fermentas
pUSER-GFP	pUC19 derivative containing a USER cloning cassette and *GFPuv*; Amp^R	This study
pUTAAG	pUSER-GFP derivative containing *tktA*, $aroF^{FBR}$ and *aroB*; Amp^R	This study
pALTAA	pALac derivative containing *tktA*, $aroF^{FBR}$ and *aroB*; Cm^R	This study
pALLACC	pALac derivative containing *aroL*, *aroA*, *aroC* and *ubiC*; Cm^R	This study
pLOI2224	Plasmid with the RK6γ origin containing a Kan^R cassette and two FRT sites, for chromosomal integration of DNA; Kan^R	Martinez-Morales et al. (1999)
pBBR1MCS3	Low-copy expression plasmid	Kovach et al. (1995)
pMBIS	pBBR1MCS3 derivative containing *ERG12*, *ERG8*, *MVD1*, *idi* and *ispA*; Tet^R	Martin et al. (2003)

et al., 2003). Growth experiments were performed in M9 medium (Sambrook et al., 1989) supplemented with 1.5% yeast extract, 3% glucose and appropriate antibiotics at 1/2 concentration, in order to reduce the initial lag phase. To prepare starter cultures for testing the engineered strains, one colony was used to inoculate a 10-mL culture, which was grown overnight and adjusted to $OD_{600}=1$. The starter cultures were then diluted ten-fold in 50 mL of medium in 250-mL shake flasks and shaken at 200 rpm and 37 °C. When the cultures reached an OD_{600} of 0.5–0.7, they were supplemented with 10 mM mevalonate as necessary and 0.5 mM IPTG.

2.2. Construction of vectors

pALac: The pALac expression vector is derived from the low-copy plasmid pACYC184. The vector was amplified using the primers pACYC184F and pACYC184R (Table S1), which anneal to regions flanking the tetracycline resistance cassette, and carry 5′-NsiI and NotI sites (pACYC184F) or 5′-NsiI and AscI sites (pACYC184R). The PCR product was digested with NsiI and DpnI and self-ligated, yielding pACCM. P_{lacZ} was amplified from *E. coli* MG1655 by colony PCR using the primers lacPAscIF and LacPPme1R1, and then with the primers LacPPMIBHI-R2 and LacPNotIR3. The P_{lacZ} cassette was then introduced into pACCM using the AscI and the NotI sites, yielding pALac.

pG-USER-GFP: In order to create a cloning vector to assemble the upper aromatic operon by the USER method (Geu-Flores et al., 2007), a module flanked by FseI, SbfI, NotI and SacI sites at the 5′ end, and by AscI and XbaI at the 3′ end, containing a PacI/Nt.BbvCI cassette, a ribosomal binding site and the coding sequence of *GFP*, was first created by PCR using the primer pair USER-GFP-F1/USER-GFP-R1 and pGFPuv as a template. The primer pairs USER-GFP-F2/USER-GFP-R2, USER-GFP-F3/USER-GFP-R3 and USER-GFP-F4/USER-GFP-R3 were then used in sequential overlapping PCR reactions. The cassette was digested with SacI and XbaI, then inserted into pUC19, yielding pUSER-GFP.

2.3. Isolation of the dps gene from Sphingomonas baekryungensis

S. baekryungensis was isolated from seawater in Advocate Bay (Nova Scotia, Canada) and identified as a high producer of CoQ_{10} (patent WO2008023264: coenzyme Q_{10} production from marine bacteria). To isolate the *dps* gene from *S. baekryungensis*, degenerate PCR primers (DPSF6 and DPSR4) were first designed based

on the conserved DPS amino acid regions LLHDDV and AFQLVD (Lee et al., 2004). A 384-bp PCR fragment was amplified from *S. baekryungensis* genomic DNA, cloned into pGEM-T Easy (Promega), and sequenced. To generate the template for inverse PCR and isolate the 5′ and 3′ regions of the *dps* gene, genomic DNA from *S. baekryungensis* was digested with NcoI, and the purified fragments were self-ligated. This template was used to amplify a 2.5-kb fragment containing the 5′ and 3′ ends of the *S. baekryungensis dps* gene, using primers DPS-iPCR-F1 and DPS-iPC-R1, designed based on the 384-bp *dps* internal fragment. The entire coding sequence of *dps* was then amplified using the primers DPSF1 and DPSR1. A synthetic version of the *dps* gene was codon-optimized for *E. coli* by GeneScript, yielding dps_o. The synthetic gene was amplified using the primers RBSDPSoKpnIF and DPSo-HindIIIR, adding an optimized RBS (Ringquist et al., 1992) at the 5′ end, and cloned into pTrc99A, yielding $pTDPS_o$ (Fig. 1B). The dps_o gene was also amplified with the primers RBSDPSBamHIF and DPSNotIR, introducing an optimized RBS at the 5′ end, and then cloned into pALac, yielding $pALDPS_o$.

2.4. Deletion of ispB from E. coli

To minimize the production of CoQ_8, the *ispB* gene was deleted from the chromosome of *E. coli* using lambda Red recombination (Datsenko and Wanner, 2000). A 1597-bp deletion cassette was amplified using primers IspBkoF and IspBkoR, and the plasmid pKD4 as a template. The reactions were treated with DpnI, and dialyzed using a 0.025 μm disc (Millipore). Cells of *E. coli* BW25113, harboring pKD46 and $pALDPS_o$ that were previously grown on LB containing L-arabinose (1 mM), were electroporated using ~475 ng of the purified DNA cassette. The Δ*ispB*::*kan* locus was transferred to MG1655 harboring $pTDPS_o$ by P1 transduction. The kanamycin marker flanked by FRT sites was removed using the helper plasmid pCP20.

2.5. Isolation of the ubiA gene from Erythrobacter sp. NAP1

The amino acid sequence of the PHB decaprenyl transferase (UbiA) from *Erythrobacter* sp. NAP1 was retrieved from GenBank (EAQ29552.1). The corresponding coding sequence was codon-optimized for *E. coli* and synthesized by DNA2.0, yielding $ubiA_o$. The optimized gene and an optimized ribosomal binding site (Ringquist et al., 1992) were inserted into $pTDPS_o$ using EcoRI and KpnI, upstream of dps_o, yielding $pTUbiA_oDPS_o$ (Fig. 1B).

2.6. Construction of synthetic upper and lower aromatic pathway operons

The coding regions of *tktA*, *aroF* and *aroB* were amplified from MG1655 genomic DNA using the primer pairs TktAF1/TktAR1, AroFF2/AroFR2 and AroBF2/AroBR2, respectively, then cloned into pGEM-T Easy, yielding pG-TktA, pG-AroF and pG-AroB. The primers AroF-PL-F1 and AroF-PL-R1 were used to introduce the base pair modification (C444T) required to introduce the Pro (148)→Leu mutation in $AroF^{FBR}$ (Weaver and Herrmann, 1990). The resulting pG-$AroF^{FBR}$ was further modified by site-directed mutagenesis using the primers AroF-T327C-F and AroF-T327C-R, in order to remove a PacI recognition site. For USER cloning (Geu-Flores et al., 2007), *tktA* was amplified using *PfuTurbo* Cx hotstart DNA polymerase (Agilent Technologies) from pG-TktA using the primers TktAUF1/TktAUR1, $aroF^{FBR}$ from pG-$AroF^{FBR}$ with the primers AroFUF2/AroFUR2 and *aroB* from pG-AroB with the primers AroBUF4/AroBUR4. The fragments were DpnI-treated, purified and mixed with pUSER-GFP pre-digested with PacI and Nt.BbvCI, as well as one unit of USER enzyme. After 20 min at 37 °C and 20 min at 25 °C, the whole reaction was transformed into *E. coli*, yielding pUTAAG. The *tktA*–$aroF^{FBR}$–*aroB* operon was amplified from pUTAAG using the primers TktAF2 and AroBR3, and then cloned into pALac, yielding pALTAA (Fig. 1B). The coding regions of *aroL*, *aroA*, *aroC* and *ubiC* were amplified from MG1655 genomic DNA using the primer pairs AroLF/AroLR, AroAF/AroAR, AroCF/AroCR and UbiCF/UbiCR, respectively. The operon was built by iterative digestion, ligation and amplification of the ligated coding regions. Briefly, the amplified coding region of *aroL* was digested with AvrII at the 3′ end while the amplified coding region of *aroA* was digested with XbaI at the 5′ end. The two digested products were then ligated, which destroys both the AvrII and XbaI sites, and subsequently amplified with AroLF and AroAR. The same procedure was repeated for the addition of the amplified *aroC* and *ubiC* to the operon. Once the entire operon was constructed, it was digested with BglII and NotI and then cloned into BamHI–NotI-digested pALac, yielding pALLACC.

2.7. Integration of the synthetic lower aromatic operon on the chromosome of E. coli

The lower aromatic pathway operon was integrated on the chromosome of *E. coli* at the *ubiC* locus by homologous recombination using the method of Martinez-Morales et al. (1999). A GFP cassette flanked by NotI and AscI sites was first cloned at the NotI site of pALLACC, and allowed the excision of an AscI-flanked synthetic operon. The operon was cloned into the AscI site of pLOI2224, yielding p24LLACC, which was subsequently electroporated into MG1655 Δ*aroL*, Δ*aroA* and Δ*aroC*. The integrated operon and the flanking kanamycin cassette were then transferred into MG1655 and MG1655 Δ*ispB*, $pTDPS_o$ by P1 transduction. The kanamycin marker was subsequently removed using pCP20, yielding MG1655, *ubiC*::LLACC (CC1.ARO2) and MG1655 Δ*ispB*, $pTDPS_o$, *ubiC*::LLACC (Fig. 1B).

2.8. Analysis of shikimic acid and para-hydroxybenzoate from culture supernatants

One-mL aliquots from *E. coli* cultures were centrifuged at 16,100*g* to remove the cells prior to HPLC analysis. The supernatant was filtered using a 13 mm 0.2 μM nylon filter (Acrodisc, VWR), and 10 μL was injected into a 1200 Series HPLC system (Agilent technologies) equipped with an Aminex HPX-87H column (Bio-Rad) heated to 65 °C. Shikimic acid (SA) was resolved using 0.1% trifluoroacetic acid (TFA) at a flow rate of 0.6 mL/min and detected with a 1200 Series UV/vis diode array detector (Agilent Technologies) at 215 nm. PHB was resolved using 0.1% TFA and 15% acetonitrile at a flow rate of 0.6 mL/min and detected at 254 nm. SA and PHB were quantified using a standard curve of authentic standards.

2.9. Quinone extraction and analysis

Cells from 1-mL aliquots of *E. coli* cultures were harvested at 16,100*g* for analysis of their quinone content. The pelleted cells were washed with 1 mL of 50 mM Tris-HCl pH 7.5, and re-suspended in 450 μL Cell Lytic B (Sigma-Aldrich). After 30 min at room temperature, a first extraction was performed with 900 μL of hexane:2-propanol (5:3). The upper phase was transferred into a new tube and a second extraction was done using 500 μL of hexane. The combined extracts were dried under an air stream, and re-suspended in 50 μL acetone. A 10-μL aliquot was injected into a 1200 Series HPLC system equipped with a ZORBAX Eclipse XDB-C18 (4.6 × 150 mm, 5 μm, Agilent technologies). The mobile phase consisted of acetonitrile (A) and ethanol (B) with the following elution profile: 0–5 min, 40% B; 5–18 min, 40–100% B; 18–32 min, 100% B. The quinones were detected at 275 nm.

CoQ_{10} was quantified using a standard curve of an authentic standard. The specific CoQ_{10} content of strain CC2.DU.1.ARO3. ISO1 was estimated by converting its OD_{600} to DCW using a standard curve. For identification by LC–MS–MS, the extracted quinones were separated by HPLC as described above, except that the mobile phase was acidified with 0.1% formic acid and 10 μM ammonium formate. The HPLC eluent was then channeled to a Quattro LC triple quadrupole mass spectrometer (Waters) with electrospray ionization in the positive mode. The source block temperature was set to 80 °C, the desolvation temperature to 200 °C and a voltage of 3.5 kV was applied to the electrospray needle. Nitrogen was used as the nebulizer, desolvation and collision gas. The precursor ions were manually selected and directed to the collision cell where they were fragmented with 30 kV or 40 kV of collision energy, depending on the metabolite.

3. Results

3.1. Cloning and functional expression of a dps in E. coli

The marine bacterium *S. baekryungensis* was identified in a screen for high producers of CoQ_{10}. Analysis of its quinone profile also revealed negligible amounts of shorter quinone species such as CoQ_9 and CoQ_8. Since previous studies have shown that the chain length of CoQ_n species is dictated by the prenyl synthase (Okada et al., 1996), we hypothesized that the DPS expressed by this species had higher stringency for DPP compared to other CoQ_{10} producers who also produce shorter coenzyme species (Okada et al., 1998; Park et al., 2005; Takahashi et al., 2003; Zahiri et al., 2006a). In order to engineer a strain highly enriched in CoQ_{10}, we cloned and expressed, in *E. coli*, the *dps* gene from *S. baekryungensis*. The nucleotide sequence encoding *dps* was codon-optimized (dps_o) in order to improve expression and the activity of DPS_o was confirmed by the accumulation of CoQ_{10}, in addition to CoQ_8, in *E. coli* MG1655 transformed with $pTDPS_o$ (Fig. 2A and B, strain CC1.D). In order to exclusively produce CoQ_{10}, the *ispB* gene was deleted from CC1.D. When comparing the quinone profile of the Δ*ispB* strain CC2.D with that of the control strain CC1.1, we observed that while CC1.1 exclusively produced octaprenyl quinones (CoQ_8 and MK-8), CC2.D produced the decaprenyl quinones CoQ_{10} and MK-10, as well as longer CoQ_{11} (Fig. 2B and C). Although some CoQ_9 were found in cells expressing both *ispB* and dps_o (strain CC1.D, Fig. 2B), we did not observe detectable amounts of CoQ_9 in CC2.D (Fig. 2C).

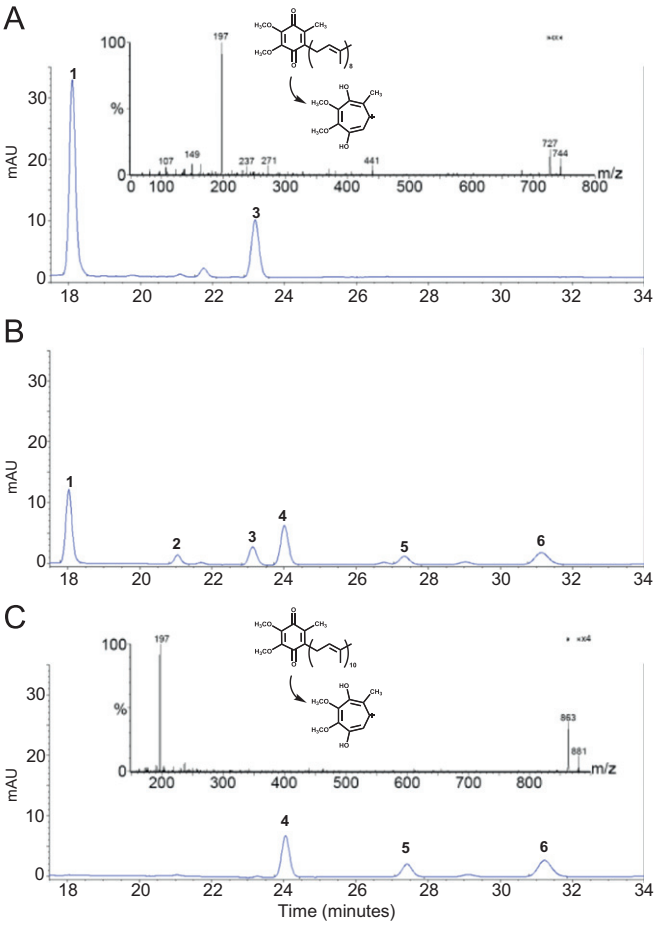

Fig. 2. HPLC profile of quinone extracts from wild-type and engineered *E. coli* strains. Strains compared are (A) CC1.1 (MG1655, pTrc99A), (B) CC1.D (MG1655, $pTDPS_o$) and (C) CC2.D (MG1655 Δ*ispB*, $pTDPS_o$). The upper panel of (A) shows the MS–MS spectrum of CoQ_8, isolated from peak 1: ammonium adduct $[M+NH_4]^+$ ($C_{49}H_{78}O_4N^+$; exact mass 744.6), protonated adduct $[M+H]^+$ ($C_{49}H_{75}O_4^+$; exact mass 727.7) and tropylium ion $[M]^+$ ($C_{10}H_{13}O_4^+$, exact mass 197.1). The upper panel of (C) shows the MS–MS spectrum of CoQ_{10}, isolated from peak 4: ammonium adduct $[M+NH_4]^+$ ($C_{59}H_{94}O_4N^+$; exact mass 880.7), protonated adduct $[M+H]^+$ ($C_{59}H_{91}O_4^+$; exact mass 863.7) and tropylium ion $[M]^+$ ($C_{10}H_{13}O_4^+$, exact mass 197.1). Labeled peaks were identified by LC–MS–MS: 1, CoQ_8; 2, CoQ_9; 3, MK-8; 4, CoQ_{10}; 5, CoQ_{11}; 6, MK-10 (MS/MS spectra shown in Fig. S1).

3.2. Deregulation of PHB biosynthesis

The benzoic head of CoQ_{10} is derived from the aromatic pathway leading to the biosynthesis of chorismate, which is then converted to PHB by the chorismate lyase, UbiC (Fig. 1A). Elevated production of PHB from glucose has previously been achieved in *E. coli* by over-expression of the rate-limiting enzymes of the aromatic pathway, along with UbiC (Barker and Frost, 2001). Based on this strategy, we created two synthetic operons, referred to as the upper and lower aromatic operons, aimed at increasing the expression of selected genes coding for enzymes of the PHB pathway (Fig. 1B).

The upper aromatic operon, designed to increase the production of shikimic acid (SA), comprises the genes coding for TktA, a feedback resistant AroF ($AroF^{FBR}$) and AroB, driven by the *lacZ* promoter P_{lacZ} (Fig. 1B). We tested its functionality by following the accumulation of SA over time in MG1655 harboring pALTAA (CC1.1.ARO1). Strain CC1.1.ARO1 produced 25 mg/L/OD_{600} of SA (Fig. 3A). To prevent the rapid conversion of SA to downstream aromatic intermediates, we expressed pALTAA in *E. coli* MG1655 Δ*aroK*Δ*aroL*, a strain deficient in shikimate kinase activity, yielding CC3.1.ARO1. Using this genetic background, the production of SA increased more than 20-fold compared to the control CC3.1 and 2.9-fold compared to CC1.1.ARO1 (Fig. 3A). The expression of the upper operon alone, however, was not sufficient to result in a significant increase in PHB production in a wild-type background compared to the control strain (Fig. 3B).

The lower aromatic operon (LACC) includes the genes coding for AroL, AroA, AroC and UbiC (Fig. 1A). The expression of these four enzymes leads to the conversion of SA to PHB. The lower operon was placed under the control of P_{lacZ}, and integrated on the chromosome downstream of the *ubiC* locus (*ubiC*::LLACC, Fig. 1B) of CC1.1 and CC1.1.ARO1, yielding CC1.1.ARO2 and CC1.1.ARO3, respectively. We did not observe an increase in PHB productivity in CC1.1.ARO2, expressing solely the lower aromatic operon, indicating that availability of SA is limiting for PHB biosynthesis (Fig. 3B). However, CC1.1.ARO3, expressing both upper and the lower operons, produced over 13 mg/L/OD_{600} of PHB, representing a 220-fold increase compared to the control CC1.1 (Fig. 3B). While up to 24 mg/L/OD_{600} of SA were produced

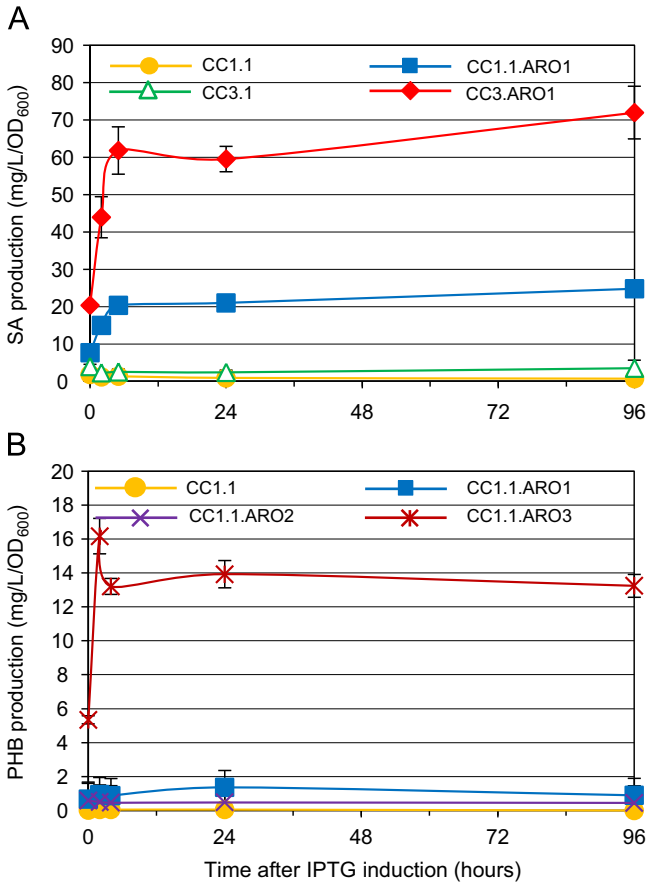

Fig. 3. Production of aromatic intermediates following the expression of the upper and lower synthetic aromatic pathway operons. Tested strains were grown in 50-mL cultures to exponential phase, and induced with 0.5 mM IPTG. Samples were taken at 0, 4, 24 and 96 h after induction in order to measure (A) the accumulation of SA in the growth media and (B) the accumulation of PHB in the growth media. Error bars show the standard deviation for duplicate biological samples.

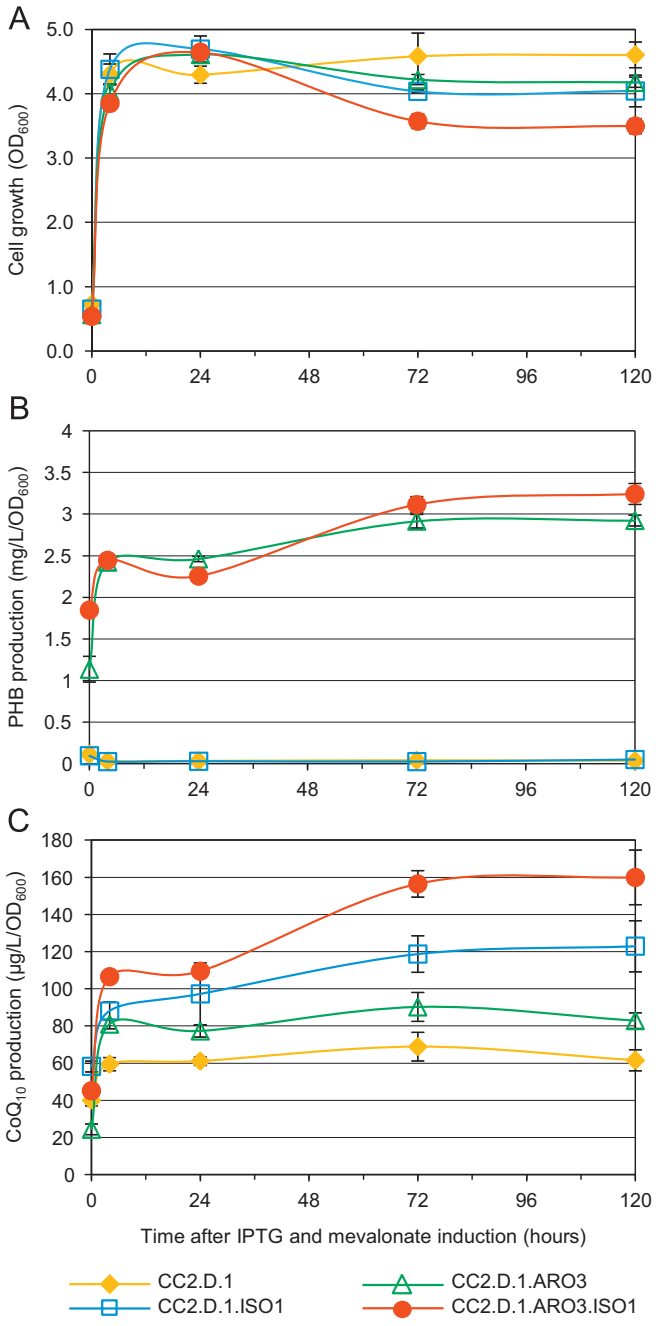

Fig. 4. Growth and metabolite production in strains expressing the upper and lower synthetic aromatic pathway operons, and/or the lower mevalonate operon. Tested strains were grown in 50-mL cultures to exponential phase, induced with 0.5 mM IPTG and 10 mM mevalonate. Samples were taken at 0, 4, 24, 72 and 120 h after induction in order to measure (A) the OD_{600}, (B) the accumulation of PHB in the growth media and (C) the intracellular concentration of CoQ_{10}. Error bars represent the standard deviation of two biological replicates.

by CC1.1.ARO1 (Fig. 3A), no residual SA was detected in the media of CC1.1.ARO3 (data not shown), suggesting that the enzymes encoded by the lower aromatic operon were able to efficiently catalyze the downstream reactions and divert carbon flux towards PHB.

3.3. *Assessment of CoQ_{10} production following the over-expression of PHB and/or FPP biosynthetic pathways*

As the availability of PHB limits the carbon flux toward CoQ_n biosynthesis (Zahiri et al., 2006b; Zhu et al., 1995), we hypothesized that a deregulation of PHB biosynthesis would translate into higher production of CoQ_{10} in an engineered *E. coli* strain. The upper and lower aromatic operons were introduced into the CoQ_{10}-producing strain CC2.D, yielding CC2.D.1.ARO3, and CoQ_{10} production was followed over time. As shown in Fig. 4C, CC2.D.1.ARO3 produced up to 83 µg/L/OD_{600} CoQ_{10}, corresponding to a 1.3-fold increase compared to the control CC2.D.1. In addition, CC2.D.1.ARO3 produced 3.2 mg/L/OD_{600} PHB (Fig. 4B), a four-fold decrease compared to CC1.1.ARO3 (Fig. 3B).

In addition to aromatic precursors, the biosynthesis of CoQ_{10} in recombinant *E. coli* is limited by the availability of DPP for the prenylation of PHB (Choi et al., 2009; Kim et al., 2006; Zahiri et al., 2006b). DPP is formed by the successive condensation of IPP with FPP (Wang and Ohnuma, 2000). In *E. coli*, the biosynthesis of these isoprenoid molecules is controlled by the MEP pathway (Fig. 1A). However, their production can be dramatically increased by the heterologous expression in *E. coli* of the typically eukaryotic mevalonate pathway (Martin et al., 2003). The pMBIS plasmid harbors the lower mevalonate operon, which includes genes coding for ERG12, ERG8 and MVD1, derived from *S. cerevisiae*, as well as the *E. coli* genes coding for Idi and IspA (Fig. 1A and B). The expression of pMBIS results in significant increases in the production of FPP and IPP in the presence of exogenously supplied mevalonate (Martin et al., 2003). In order to increase the

availability of FPP for CoQ_{10} biosynthesis, we transformed pMBIS into CC2.D, yielding CC2.D.1.ISO1. The expression of this construct in CC2.D.1.ISO1 resulted in a 2-fold increase in CoQ_{10} content (123 μg/L/OD_{600}) over the control CC2.D.1 (Fig. 4C).

Prompted by these results, we hypothesized that an even greater increase in CoQ_{10} production would be observed if both the PHB and the isoprenoid pathways were over-expressed in the same strain. The engineered aromatic and lower mevalonate pathways were introduced in strain CC2.D, resulting in strain CC2.D.1.ARO3.ISO1, and the latter was tested for CoQ_{10} production. As shown by Fig. 4C, CC2.D.1.ARO3.ISO1 reached a CoQ_{10} content of 160 μg/L/OD_{600}, a 2.6-fold increase over the control CC2.D.1. This suggests that both aromatic and isoprenoid precursors are rate-limiting for CoQ_{10} biosynthesis and that both of these pathways can be simultaneously engineered in *E. coli* to produce a high CoQ_{10}-producing strain without the need for feeding the PHB precursor. Only a slight difference was observed in PHB accumulation between CC2.D.1.ARO3.ISO1 and CC2.D.1.ARO3 (Fig. 4B).

In addition to its increased CoQ_{10} content, CC2.D.1.ARO3.ISO1 had elevated concentrations of an unknown molecule, which eluted 1 min before CoQ_{10} on the HPLC chromatogram (Fig. 5A). Analysis of this unknown compound by LC–MS–MS revealed a precursor ion at m/z=792 and product ions at m/z=775 and m/z=107 (Fig. 5B, Fig. S2), characteristic of the ammonium adduct $[M+NH_4]^+$, the protonated ion $[M+H]^+$ and the tropylium ion $[M]^+$, respectively, derived from the CoQ_{10} intermediate, 2-decaprenylphenol (10P-Ph) (Cox et al., 1969; Hsu et al., 1996; Matsumura et al., 1983). 10P-Ph is the second intermediate of the ubiquinone pathway, formed by the hydroxylation of 3-decaprenyl-4-hydroxybenzoate (10P-HB) (Fig. 1A) (Alexander and Young, 1978). Although the unavailability of a suitable standard precluded the quantification of this compound, a comparison of its relative abundance between different strains revealed that CC2.D.1.ARO3.ISO1 accumulated 14 times more 10P-Ph than CC2.D.1.ISO1, while CC2.D.1.ARO3 did not accumulate detectable levels of this intermediate (Fig. 5C).

3.4. Over-expression of a para-hydroxybenzoate decaprenyl transferase from Erythrobacter sp. NAP1

Although we observed an increase in CoQ_{10} production following the over-expression of both the aromatic and the lower mevalonate pathways in CC2.D.1.ARO3.ISO1, we found that PHB accumulation levels by the latter and by CC2.D.1.ARO3 were almost similar (Fig. 4B). The entry of PHB and DPP into the ubiquinone pathway is brought about by the PHB prenyltransferase, UbiA, condensing DPP and PHB to form 10P-HB (Fig. 1A). It is possible that the limited flux of PHB towards the ubiquinone pathway in CC2.D.1.ARO3.ISO1 reflects a bottleneck at the PHB prenylation step carried out by UbiA. We hypothesized that microorganisms naturally accumulating high levels of CoQ_{10} might express PHB decaprenyl transferases of increased efficiency. In order to overcome a potential bottleneck at the PHB prenylation step in our engineered *E. coli* strains, we expressed a codon-optimized version of *ubiA* (*ubiA*$_o$) that was isolated from the CoQ_{10}-producing marine bacterium *Erythrobacter* sp. NAP1 (Fig. 1B). The plasmid pTUbiA$_o$DPS$_o$ was expressed in a Δ*ispB* background along with the aromatic operons, the pMBIS plasmid or the corresponding empty vectors, yielding strains CC2.DU.1, CC2.DU.1.ARO3, CC2.DU.1.ISO1 and CC2.DU.1.ARO3.ISO1 (Table 1).

The heterologous expression of *ubiA*$_o$ in CC2.DU.1.ISO1, CC2.DU.1.ARO3, CC2.DU.1.ARO3.ISO1 and CC2.DU.1 was associated with an extended initial lag phase and with reduced growth (Fig. 6A). The accumulation of PHB was 3.6-fold higher in CC2.DU.1.ARO3 than in CC2.DU.1.ARO3.ISO1 suggesting that the latter was either producing less PHB, or that PHB was metabolized into other molecules (Fig. 6B). Consistent with the hypothesis that the over-expression of UbiA$_o$ favors the production of CoQ_{10} when high concentrations of aromatic and isoprenoid precursors are available, CC2.DU.ARO3.ISO1 achieved the highest CoQ_{10} content amongst the strains tested. As shown by Fig. 6C, CC2.DU.ARO3.ISO1 produced up to 213 μg/L/OD_{600}, compared to 138 μg/L/OD_{600} for CC1.D.1.ARO3.ISO1 (Fig. 6C). The specific CoQ_{10} content for CC2.DU.ARO3.ISO1 was estimated to be 0.8 mg/g DCW. In contrast to its higher CoQ_{10} content, CC2.DU.ARO3.ISO1 produced 1.8-fold less 10P-Ph than CC1.D.1.ARO3.ISO1 (Fig. 6D). This suggests that the over-expression of UbiA$_o$ reduces the accumulation of 10P-Ph in CC2.DU.ARO3.ISO1, and favors the accumulation of CoQ_{10}.

The over-expression of UbiA$_o$ along with the lower mevalonate pathway in CC2.DU.ISO1 resulted in the accumulation of a new compound, which eluted from the HPLC column 4.5 min before CoQ_{10} (Fig. 7A). Analysis of this molecule by LC–MS–MS revealed

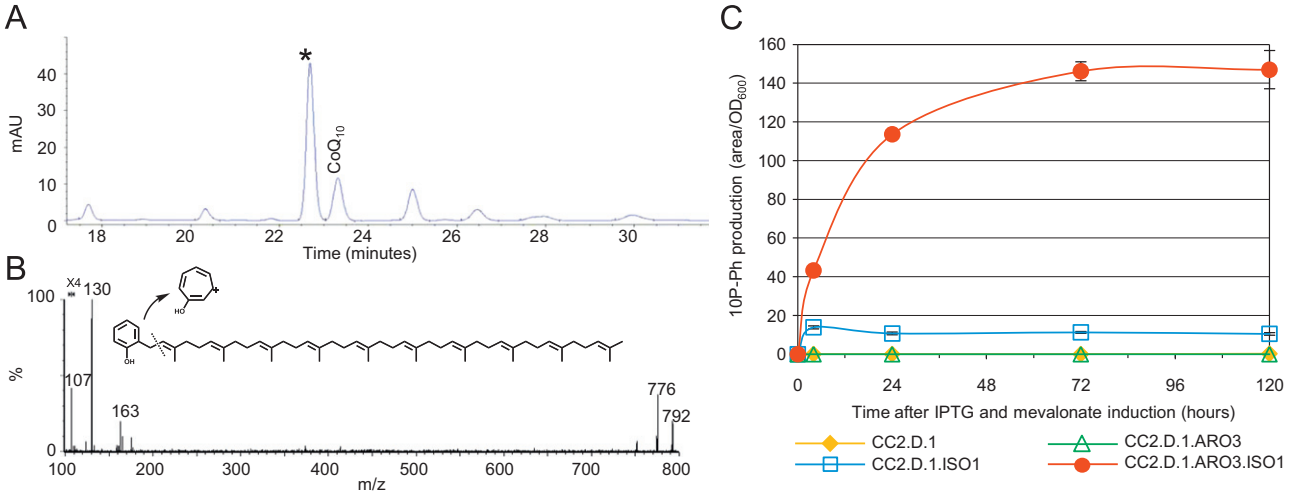

Fig. 5. Production of 2-decaprenylphenol (10P-Ph) by CC2.D.1.ARO3.ISO1. The production of a ubiquinone pathway intermediate, 10P-Ph, was characterized in CC1.D.1.ARO3.ISO1. (A) HPLC chromatogram of extracted quinones from CC1.D.1.ARO3.ISO1, 24 h after induction with 0.5 mM IPTG and 10 mM mevalonate. The 10P-Ph peak is labeled with a star. (B) LC–MS–MS spectrum of 10P-Ph. The fragmented precursor ion yielded an ammonium adduct $[M+NH_4]^+$ ($C_{56}H_{90}ON^+$, exact mass 792.7), a protonated ion $[M+H]^+$ ($C_{56}H_{87}O^+$, exact mass 775.7) and a tropylium ion $[M]^+$ ($C_7H_7O_+$, exact mass 107.0). The identity of 10P-Ph was confirmed in parallel on a LTQ Orbitrap Velos MS (Fig. S2). (C) Time-course of 10P-Ph production in 50-mL cultures, after induction with 0.5 mM IPTG and 10 mM mevalonate. Error bars represent the standard deviation of two biological replicates.

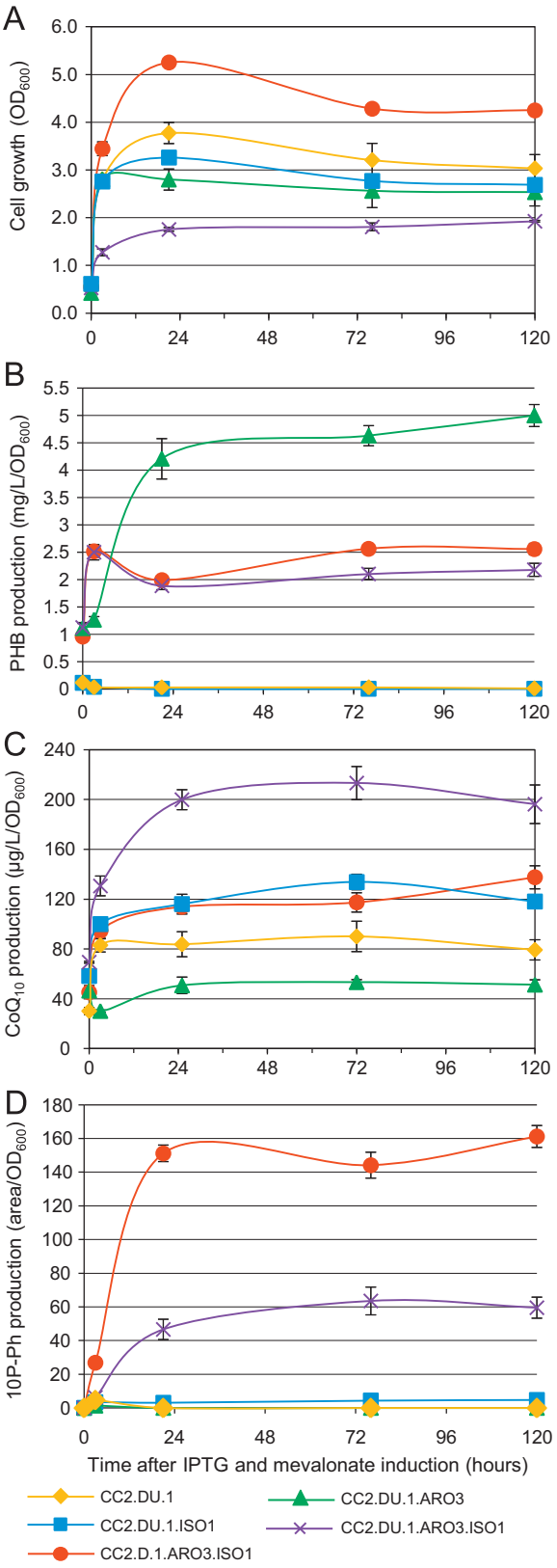

Fig. 6. Growth and metabolite production in strains expressing the upper and lower aromatic operons, the lower mevalonate operon and/or the PHB prenyltransferase $UbiA_o$. Tested strains were grown in 50-mL cultures to exponential phase, then induced with 0.5 mM IPTG and 10 mM mevalonate. Samples were taken at 0, 3, 25, 72 and 120 h after induction in order to measure (A) the OD_{600}, (B) the accumulation of PHB in the growth media, (C) the intracellular concentration of CoQ_{10} and (D) the intracellular concentration of 10P-Ph. Error bars represent the standard deviation of two biological replicates.

a precursor ion of *m*/*z* 818 and a product ion of *m*/*z* 150, corresponding to the protonated precursor ion and to the tropylium product ion, respectively, of 3-decaprenyl-4-aminobenzoate (10P-AB) (Fig. 7B) (Hamilton and Cox, 1971; Marbois et al., 2010). The accumulation of this hybrid metabolite has never been observed in a CoQ_{10}-producing *E. coli* strain, but has been reported in *E. coli* when UbiA uses *para*-aminobenzoate (PABA) as its substrate, typically when the production of PHB is defective (Hamilton and Cox, 1971; Lawrence et al., 1974). Interestingly, none of the other strains tested produced measurable amounts of 2-decaprenyl-4-aminobenzoate (Fig. 7C).

4. Discussion

The use of *E. coli* as a host for the production of CoQ_{10} offers several advantages, including the capacity to optimize metabolic pathways playing roles in its production. In this research we sought to systematically investigate how different approaches, both hypothesized and published (Zahiri et al., 2006b; Zhang et al., 2007), affect the flux of carbon towards CoQ_{10} in recombinant *E. coli*. As such, we set out to increase flux of precursor molecules to the ubiquinone pathway by simultaneously increasing the production of both the aromatic and isoprenoid precursor molecules, as well as increasing the PHB prenyltransferase (UbiA) activity.

Strain CC2.DU.1.ARO3.ISO1, which combines the over-expression of isoprenoid and aromatic precursors with that of DPS_o and $UbiA_o$, achieved a 3.2-fold increase in CoQ_{10} content compared to the control strain CC2.D.1, over-expressing DPS_o alone (Figs. 6C and 4C). This indicates that the increased flux of precursors towards the ubiquinone pathway can significantly improve CoQ_{10} content in engineered *E. coli*. Nevertheless, the specific CoQ_{10} content obtained in CC2.DU.1.ARO3.ISO1 (0.8 mg/g DCW) was inferior to those previously reported following the over-expression of a DPS and of a foreign mevalonate pathway in *E. coli* (Zahiri et al., 2006b). However, the latter report describes considerable increases in CoQ_{10} content following optimization of the growth medium, which was beyond the scope of our study (Zahiri et al., 2006b). Additionally, the 213 µg/L/OD_{600} CoQ_{10} obtained in CC2.DU.1.ARO3.ISO1 represents 2% of the theoretical yield from PHB in our strain (Fig. 6), indicating that bottlenecks still prohibit maximum CoQ_{10} content. We also found that the expression of $pTUbiA_oDPS_o$ is toxic to our engineered strains (Fig. 6A). Replacement of the *Erythrobacter ubiA*$_o$ by the *E. coli ubiA* did not alleviate this reduced growth phenotype (data not shown). While growth defects have not been reported in other accounts of UbiA over-expression (Ohara et al., 2004; Zhang et al., 2007, 2006; Zhu et al., 1995), the plasmid copy number, promoter strength and growth conditions are not identical to those described in this study. In order to attenuate the toxicity associated with $UbiA_o$, it may be necessary to lower the copy-number of the expression plasmid, or to decrease the translation rate of the protein by lowering the incubation temperature after induction (Wagner et al., 2006). Alternatively, it is possible that the observed phenotype is due to the accumulation of a detrimental intermediate created by an imbalance in enzyme activities throughout the pathway. Therefore, further optimization of the expression levels of different enzymes may be required to balance carbon flux and relieve growth defects in strains expressing $UbiA_o$ (Pitera et al., 2007).

The recombinant expression of the synthetic upper and lower aromatic pathway operons significantly increased the production of PHB in our engineered strains (Figs. 4B and 6B). Yet, it is uncertain whether the PHB produced remains at a high concentration in the cytoplasm, where it can readily be used by UbiA, or if it is rapidly excreted into the growth media. It may be possible

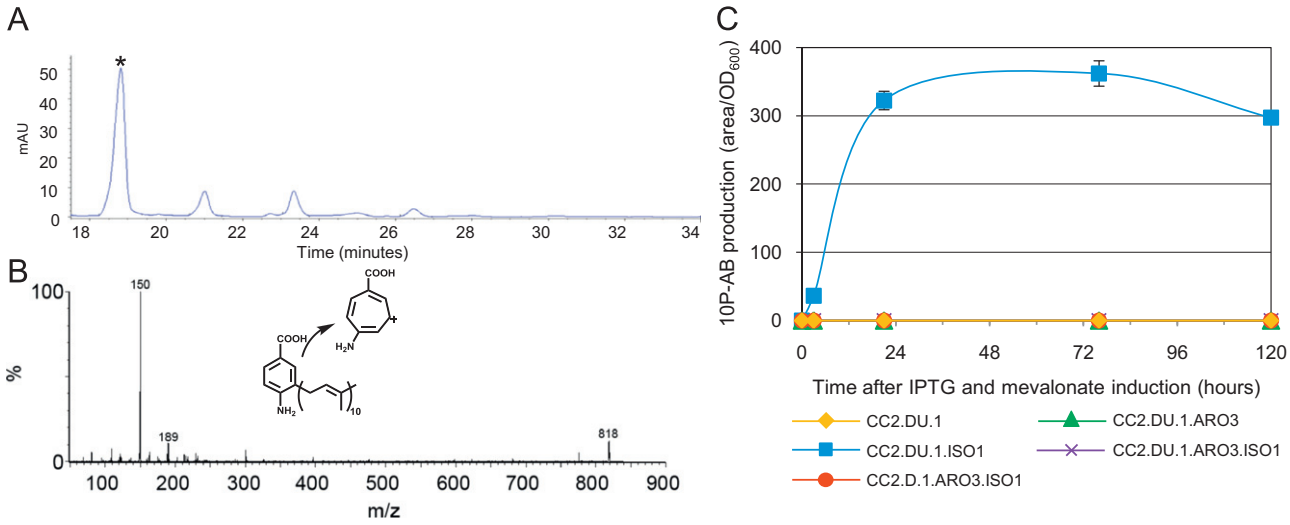

Fig. 7. Production of 3-decaprenyl-4-aminobenzoate (10P-AB) by CC2.DU.1.ISO1. The production of 10P-AB was characterized in CC2.DU.1.ISO1. (A) HPLC chromatogram of extracted quinones from CC2.DU.1.ISO1, 24 h after induction with 0.5 mM IPTG and 10 mM mevalonate. The 10P-AB peak is labeled with a star. (B) LC–MS–MS spectrum of 10P-AB. The fragmented precursor ion yielded a protonated ion $[M+H]^+$ ($C_{57}H_{88}NO_2^+$, exact mass 818.7), and a tropylium ion $[M]^+$ ($C_8H_8NO_2^+$, exact mass 150.1). (C) Time-course of 10P-AB production in 50-mL cultures, after induction with 0.5 mM IPTG and 10 mM mevalonate. Error bars represent the standard deviation of two biological replicates.

to further increase flux towards PHB by abolishing the expression of enzymes competing for its precursor, chorismate (Barker and Frost, 2001; Nakajima et al., 2009). Exogenous PHB up-regulates *aaeXAB* in *E. coli*, an operon coding for efflux proteins involved in the excretion of PHB out of the cell (Van Dyk et al., 2004). Ensuring the availability of PHB to UbiA in the cytoplasm, rather than maximizing its production, may be key to further improving CoQ_{10} contents in *E. coli*.

The introduction of the pMBIS plasmid aimed at alleviating bottlenecks resulting from the rate-limiting supply of isoprenoid precursors (Kim et al., 2006; Zahiri et al., 2006b). Although, the expression of the enzymes encoded by the MBIS operon allows for the production of high levels of FPP and IPP/DMAPP (Martin et al., 2003), DPS_o may not fully convert these precursor molecules into DPP. We have shown that complementation of the Δ*ispB* deletion strain, an essential gene for *E. coli* (Okada et al., 1997b), with dps_o is sufficient to restore growth. However, assuming similar extinction coefficients between CoQ_8 and CoQ_{10}, the accumulation of CoQ_{10} in strain CC2.D is less than the accumulation of CoQ_8 in the wild-type strain MG1655 (Fig. 2), suggesting that the catalytic properties of DPS_o may be inferior to those of IspB. DPS_o activity also leads to the production of CoQ_{11}, suggesting that this particular enzyme produces *E*-undecaprenyl diphosphate in addition to DPP. While the heterologous expression of several DPS proteins has been documented to result in the production of shorter *E*-polyprenyl species in addition to DPP, as inferred by the accumulation of a mixture of CoQ_{10}, CoQ_9 and CoQ_8 (Okada et al., 1997a; Park et al., 2005; Takahashi et al., 2003; Zahiri et al., 2006a), the biosynthesis of *E*-undecaprenyl diphosphate and of CoQ_{11} has, to the best of our knowledge, never before been reported in *E. coli*. A more complete characterization and optimization of DPS_o, or an investigation into alternative DPS enzymes with variable kinetic properties (Ma et al., 2011), will be necessary to ensure that the supply of DPP is not limiting CoQ_{10} production.

The enhanced production of aromatic and isoprenoid molecules in CC2.D.1.ARO3.ISO1 and CC2.DU.1.ARO3.ISO1 led to the accumulation of 10P-Ph, an intermediate of the ubiquinone pathway (Figs. 5C and 6D). While the accumulation of 10P-Ph and octaprenylphenol (8P-Ph) as a by-product of CoQ_{10} and CoQ_8 biosynthesis has been documented in anaerobic cultures of *Paracoccus denitrificans* (Matsumura et al., 1983) and *E. coli* (Alexander and Young, 1978), respectively, this is the first time that the accumulation of 10P-Ph is reported in an *E. coli* strain engineered to produce CoQ_{10}. The intermediate 8P-Ph accumulates in a number of *E. coli* strains carrying mutations in genes of the ubiquinone pathway, such as *ubiB*, *ubiH* and *ubiG* (Alexander and Young, 1978; Hsu et al., 1996; Poon et al., 2000; Young et al., 1973). When flux through the ubiquinone pathway increases as a result of the augmented production of aromatic and isoprenoid precursors, the activity of one of the above-mentioned Ubi enzymes may become rate-limiting, resulting in the accumulation of 10P-Ph. The strain CC2.DU.1.ARO3.ISO1 had a lower 10P-Ph content compared to CC2.D.1.ARO3.ISO1, along with higher CoQ_{10} production (Fig. 6D), suggesting that increasing PHB prenyltransferase activity improves the flux within the ubiquinone pathway, downstream of the decarboxylation step. It is possible that one or more enzymes of the ubiquinone pathway are dependent on UbiA for their activity. Studies in *S. cerevisiae* provide compelling evidence for the existence of a multi-protein complex involved in the production of CoQ_6 (Gin and Clarke, 2005; Gin et al., 2003; Johnson et al., 2005; Tran et al., 2006). It is hypothesized that Coq2p, the homolog of UbiA, does not physically interact with the complex, but that its product, 3-hexaprenyl-4-hydroxybenzoate (6P-HB), plays a role in the assembly and/or stability of the complex (Hsieh et al., 2007; Hsu et al., 2000; Suzuki et al., 1994). While physical interactions between Ubi proteins have not yet been demonstrated in *E. coli*, early literature on the ubiquinone pathway hints at the existence of a soluble multi-protein complex capable of converting 8P-Ph to CoQ_8 (Knoell, 1979, 1981). Increasing the expression of the members of this protein complex will be key to further channeling 10P-Ph towards CoQ_{10} in strains CC2.D.1.ARO3.ISO1 and in CC2.DU.1.ARO3.ISO1.

The increased production of isoprenoids, coupled with the over-expression of $UbiA_o$ in CC2.DU.1.ISO1, led to the accumulation of a new metabolite, 10P-AB (Fig. 7). This compound does not have a known biological function in *E. coli*, but accumulates in a mutant lacking chorismate lyase activity when grown in the presence of PABA (Hamilton and Cox, 1971). Growth inhibition of *E. coli* by high concentrations of exogenous PABA can be reversed by the addition of PHB (Davis, 1951), suggesting that PABA may act as a competitive inhibitor of UbiA by displacing

PHB within the active site of UbiA. In CC2.DU.1.ISO1, the increased PHB prenyl transferase ($UbiA_o$) activity combined with the higher availability of DPP may result in the exhaustion of the endogenously produced PHB, causing UbiA/$UbiA_o$ to accept PABA as an alternative substrate. In *S. cerevisiae*, PABA can also be used as a substrate for Coq2p and further channeled through the ubiquinone pathway (Marbois et al., 2010). Based on the results of this study, it would appear that while UbiA can use PABA to form 10P-AB, the latter compound is not recognized by the *E. coli* decarboxylases UbiD and UbiX, therefore leading to an accumulation of this metabolite in CC2.DU.1.ISO1. These findings demonstrate the importance of precursor stoichiometry in the metabolic engineering of complex multi-branch pathways.

In summary, this report describes the development of a CoQ_{10}-producing *E. coli* strain engineered to over-produce aromatic and isoprenoid precursors and to have increased PHB prenyl transferase activity. It is the first instance where both precursor pathways have been over-expressed and genetically deregulated in combination with the over-expression of the enzyme bridging these two pathways, UbiA. The results presented in this study highlight the existence of previously unreported bottlenecks in CoQ_{10} overproduction in *E. coli*, and will enhance our ability to design further improvements of this system.

Acknowledgments

This work was supported by an NSERC Strategic Research Grant and Ocean Nutrition Canada. The authors would like to acknowledge Josh Levin and David Papadopoli for their contributions, and Alain Tessier for help with the LC–MS–MS experiments. C.P.C. is the recipient of an NSERC Canada Graduate Scholarship and V.J.J.M. is supported by a Canada Research Chair.

Appendix A. Supporting information

Supplementary data associated with this article can be found in the online version at doi:10.1016/j.ymben.2011.09.009.

References

Alexander, K., Young, I.G., 1978. Alternative hydroxylases for the aerobic and anaerobic biosynthesis of ubiquinone in *Escherichia coli*. Biochemistry 17, 4750–4755.

Baba, T., Ara, T., Hasegawa, M., Takai, Y., Okumura, Y., Baba, M., Datsenko, K.A., Tomita, M., Wanner, B.L., Mori, H., 2006. Construction of *Escherichia coli* K-12 in-frame, single-gene knockout mutants: the Keio collection. Mol. Syst. Biol. 2 2006 0008.

Bader, M.W., Xie, T., Yu, C.A., Bardwell, J.C., 2000. Disulfide bonds are generated by quinone reduction. J. Biol. Chem. 275, 26082–26088.

Barker, J.L., Frost, J.W., 2001. Microbial synthesis of p-hydroxybenzoic acid from glucose. Biotechnol. Bioeng. 76, 376–390.

Choi, G.-S., Kim, Y.-S., Seo, J.-H., Ryu, Y.-W., 2005. Restricted electron flux increases coenzyme Q_{10} production in *Agrobacterium tumefaciens* ATCC4452. Process Biochem. 40, 3225–3229.

Choi, J.H., Ryu, Y.W., Park, Y.C., Seo, J.H., 2009. Synergistic effects of chromosomal *ispB* deletion and *dxs* overexpression on coenzyme Q(10) production in recombinant *Escherichia coli* expressing *Agrobacterium tumefaciens dps* gene. J. Biotechnol. 144, 64–69.

Cox, G.B., Young, I.G., McCann, L.M., Gibson, F., 1969. Biosynthesis of ubiquinone in *Escherichia coli* K-12: location of genes affecting the metabolism of 3-octaprenyl-4-hydroxybenzoic acid and 2-octaprenylphenol. J. Bacteriol. 99, 450–458.

Datsenko, K.A., Wanner, B.L., 2000. One-step inactivation of chromosomal genes in *Escherichia coli* K-12 using PCR products. Proc. Natl. Acad. Sci. USA 97, 6640–6645.

Davis, B.D., 1951. Inhibition of *Escherichia coli* by p-aminobenzoic acid and its reversal by p-hydroxybenzoic acid. J. Exp. Med. 94, 243–254.

Echtay, K.S., Winkler, E., Klingenberg, M., 2000. Coenzyme Q is an obligatory cofactor for uncoupling protein function. Nature 408, 609–613.

Geu-Flores, F., Nour-Eldin, H.H., Nielsen, M.T., Halkier, B.A., 2007. USER fusion: a rapid and efficient method for simultaneous fusion and cloning of multiple PCR products. Nucleic Acids Res. 35, e55.

Gin, P., Clarke, C.F., 2005. Genetic evidence for a multi-subunit complex in coenzyme Q biosynthesis in yeast and the role of the Coq1 hexaprenyl diphosphate synthase. J. Biol. Chem. 280, 2676–2681.

Gin, P., Hsu, A.Y., Rothman, S.C., Jonassen, T., Lee, P.T., Tzagoloff, A., Clarke, C.F., 2003. The *Saccharomyces cerevisiae* COQ6 gene encodes a mitochondrial flavin-dependent monooxygenase required for coenzyme Q biosynthesis. J. Biol. Chem. 278, 25308–25316.

Gu, S.B., Yao, J.M., Yuan, Q.P., Xue, P.J., Zheng, Z.M., Yu, Z.L., 2006. Kinetics of *Agrobacterium tumefaciens* ubiquinone-10 batch production. Process Biochem. 41, 1908–1912.

Ha, S.J., Kim, S.Y., Seo, J.H., Jeya, M., Zhang, Y.W., Ramu, T., Kim, I.W., Lee, J.K., 2009. Ca^{2+} increases the specific coenzyme Q_{10} content in *Agrobacterium tumefaciens*. Bioprocess Biosyst. Eng. 32, 697–700.

Ha, S.J., Kim, S.Y., Seo, J.H., Moon, H.J., Lee, K.M., Lee, J.K., 2007a. Controlling the sucrose concentration increases coenzyme Q_{10} production in fed-batch culture of *Agrobacterium tumefaciens*. Appl. Microbiol. Biotechnol. 76, 109–116.

Ha, S.J., Kim, S.Y., Seo, J.H., Oh, D.K., Lee, J.K., 2007b. Optimization of culture conditions and scale-up to pilot and plant scales for coenzyme Q(10) production by *Agrobacterium tumefaciens*. Appl. Microbiol. Biotechnol. 74, 974–980.

Hamilton, J.A., Cox, G.B., 1971. Ubiquinone biosynthesis in *Escherichia coli* K-12. Accumulation of an octaprenol, farnesylfarnesylgeraniol, by a multiple aromatic auxotroph. Biochem. J. 123, 435–443.

Harker, M., Bramley, P.M., 1999. Expression of prokaryotic 1-deoxy-D-xylulose-5-phosphatases in *Escherichia coli* increases carotenoid and ubiquinone biosynthesis. FEBS Lett. 448, 115–119.

Hodgson, J.M., Watts, G.F., Playford, D.A., Burke, V., Croft, K.D., 2002. Coenzyme Q_{10} improves blood pressure and glycaemic control: a controlled trial in subjects with type 2 diabetes. Eur. J. Clin. Nutr. 56, 1137–1142.

Hsieh, E.J., Gin, P., Gulmezian, M., Tran, U.C., Saiki, R., Marbois, B.N., Clarke, C.F., 2007. *Saccharomyces cerevisiae* Coq9 polypeptide is a subunit of the mitochondrial coenzyme Q biosynthetic complex. Arch. Biochem. Biophys. 463, 19–26.

Hsu, A.Y., Do, T.Q., Lee, P.T., Clarke, C.F., 2000. Genetic evidence for a multi-subunit complex in the O-methyltransferase steps of coenzyme Q biosynthesis. Biochim. Biophys. Acta 1484, 287–297.

Hsu, A.Y., Poon, W.W., Shepherd, J.A., Myles, D.C., Clarke, C.F., 1996. Complementation of coq3 mutant yeast by mitochondrial targeting of the *Escherichia coli* UbiG polypeptide: evidence that UbiG catalyzes both O-methylation steps in ubiquinone biosynthesis. Biochemistry 35, 9797–9806.

Ingledew, W.J., Poole, R.K., 1984. The respiratory chains of *Escherichia coli*. Microbiol. Rev. 48, 222–271.

Inui, M., Ooe, M., Fujii, K., Matsunaka, H., Yoshida, M., Ichihashi, M., 2008. Mechanisms of inhibitory effects of CoQ_{10} on UVB-induced wrinkle formation in vitro and in vivo. Biofactors 32, 237–243.

Johnson, A., Gin, P., Marbois, B.N., Hsieh, E.J., Wu, M., Barros, M.H., Clarke, C.F., Tzagoloff, A., 2005. COQ9, a new gene required for the biosynthesis of coenzyme Q in *Saccharomyces cerevisiae*. J. Biol. Chem. 280, 31397–31404.

Kien, N.B., Kong, I.S., Lee, M.G., Kim, J.K., 2010. Coenzyme Q_{10} production in a 150-l reactor by a mutant strain of *Rhodobacter sphaeroides*. J. Ind. Microbiol. Biotechnol. 37, 521–529.

Kim, S.J., Kim, M.D., Choi, J.H., Kim, S.Y., Ryu, Y.W., Seo, J.H., 2006. Amplification of 1-deoxy-D-xyluose 5-phosphate (DXP) synthase level increases coenzyme Q_{10} production in recombinant *Escherichia coli*. Appl. Microbiol. Biotechnol. 72, 982–985.

Knoell, H.E., 1979. Isolation of a soluble enzyme complex comprising the ubiquinone-8 synthesis apparatus from the cytoplasmic membrane of *Escherichia coli*. Biochem. Biophys. Res. Commun. 91, 919–925.

Knoell, H.E., 1981. Stand-by position of the dioxygen-dependent ubiquinone-8 synthesis apparatus in anaerobically grown *Escherichia coli* K-12. FEMS Microbiol. Lett. 10, 59–62.

Kovach, M.E., Elzer, P.H., Hill, D.S., Robertson, G.T., Farris, M.A., Roop 2nd, R.M., Peterson, K.M., 1995. Four new derivatives of the broad-host-range cloning vector pBBR1MCS, carrying different antibiotic-resistance cassettes. Gene 166, 175–176.

Kroger, A., Klingenberg, M., 1973. Further evidence for the pool function of ubiquinone as derived from the inhibition of the electron transport by antimycin. Eur. J. Biochem. 39, 313–323.

Lass, A., Sohal, R.S., 1998. Electron transport-linked ubiquinone-dependent recycling of alpha-tocopherol inhibits autooxidation of mitochondrial membranes. Arch. Biochem. Biophys. 352, 229–236.

Lawrence, J., Cox, G.B., Gibson, F., 1974. Biosynthesis of ubiquinone in *Escherichia coli* K-12: biochemical and genetic characterization of a mutant unable to convert chorismate into 4-hydroxybenzoate. J. Bacteriol. 118, 41–45.

Lee, J.K., Her, G., Kim, S.Y., Seo, J.H., 2004. Cloning and functional expression of the *dps* gene encoding decaprenyl diphosphate synthase from *Agrobacterium tumefaciens*. Biotechnol. Prog. 20, 51–56.

Ma, S.M., Garcia, D.E., Redding-Johanson, A.M., Friedland, G.D., Chan, R., Batth, T.S., Haliburton, J.R., Chivian, D., Keasling, J.D., Petzold, C.J., Soon Lee, T., Chhabra, S.R., 2011. Optimization of a heterologous mevalonate pathway through the use of variant HMG-CoA reductases. Metab. Eng. 13, 588–597.

Marbois, B., Xie, L.X., Choi, S., Hirano, K., Hyman, K., Clarke, C.F., 2010. para-aminobenzoic acid is a precursor in coenzyme Q6 biosynthesis in *Saccharomyces cerevisiae*. J. Biol. Chem. 285, 27827–27838.

Martin, S.F., Buron, I., Espinosa, J.C., Castilla, J., Villalba, J.M., Torres, J.M., 2007. Coenzyme Q and protein/lipid oxidation in a BSE-infected transgenic mouse model. Free Radical Biol. Med. 42, 1723–1729.

Martin, V.J., Pitera, D.J., Withers, S.T., Newman, J.D., Keasling, J.D., 2003. Engineering a mevalonate pathway in *Escherichia coli* for production of terpenoids. Nat. Biotechnol. 21, 796–802.

Martinez-Morales, F., Borges, A.C., Martinez, A., Shanmugam, K.T., Ingram, L.O., 1999. Chromosomal integration of heterologous DNA in *Escherichia coli* with precise removal of markers and replicons used during construction. J. Bacteriol. 181, 7143–7148.

Matsumura, M., Kobayashi, T., Aiba, S., 1983. Anaerobic production of ubiquinone-10 by *Paracoccus denitrificans*. Appl. Microbiol. Biotechnol. 17, 85–89.

Nakajima, M., Nishino, Y., Tamura, M., Mase, K., Masai, E., Otsuka, Y., Nakamura, M., Sato, K., Fukuda, M., Shigehara, K., Ohara, S., Katayama, Y., Kajita, S., 2009. Microbial conversion of glucose to a novel chemical building block, 2-pyrone-4,6-dicarboxylic acid. Metab. Eng. 11, 213–220.

Ohara, K., Kokado, Y., Yamamoto, H., Sato, F., Yazaki, K., 2004. Engineering of ubiquinone biosynthesis using the yeast coq2 gene confers oxidative stress tolerance in transgenic tobacco. Plant J. 40, 734–743.

Okada, K., Kainou, T., Tanaka, K., Nakagawa, T., Matsuda, H., Kawamukai, M., 1998. Molecular cloning and mutational analysis of the *ddsA* gene encoding decaprenyl diphosphate synthase from *Gluconobacter suboxydans*. Eur. J. Biochem. 255, 52–59.

Okada, K., Kamiya, Y., Zhu, X., Suzuki, K., Tanaka, K., Nakagawa, T., Matsuda, H., Kawamukai, M., 1997a. Cloning of the *sdsA* gene encoding solanesyl diphosphate synthase from *Rhodobacter capsulatus* and its functional expression in *Escherichia coli* and *Saccharomyces cerevisiae*. J. Bacteriol. 179, 5992–5998.

Okada, K., Minehira, M., Zhu, X., Suzuki, K., Nakagawa, T., Matsuda, H., Kawamukai, M., 1997b. The *ispB* gene encoding octaprenyl diphosphate synthase is essential for growth of *Escherichia coli*. J. Bacteriol. 179, 3058–3060.

Okada, K., Suzuki, K., Kamiya, Y., Zhu, X., Fujisaki, S., Nishimura, Y., Nishino, T., Nakagawa, T., Kawamukai, M., Matsuda, H., 1996. Polyprenyl diphosphate synthase essentially defines the length of the side chain of ubiquinone. Biochim. Biophys. Acta 1302, 217–223.

Park, Y.C., Kim, S.J., Choi, J.H., Lee, W.H., Park, K.M., Kawamukai, M., Ryu, Y.W., Seo, J.H., 2005. Batch and fed-batch production of coenzyme Q_{10} in recombinant *Escherichia coli* containing the decaprenyl diphosphate synthase gene from *Gluconobacter suboxydans*. Appl. Microbiol. Biotechnol. 67, 192–196.

Pitera, D.J., Paddon, C.J., Newman, J.D., Keasling, J.D., 2007. Balancing a heterologous mevalonate pathway for improved isoprenoid production in *Escherichia coli*. Metab. Eng. 9, 193–207.

Poon, W.W., Davis, D.E., Ha, H.T., Jonassen, T., Rather, P.N., Clarke, C.F., 2000. Identification of *Escherichia coli ubiB*, a gene required for the first monooxygenase step in ubiquinone biosynthesis. J. Bacteriol. 182, 5139–5146.

Ringquist, S., Shinedling, S., Barrick, D., Green, L., Binkley, J., Stormo, G.D., Gold, L., 1992. Translation initiation in *Escherichia coli*: sequences within the ribosome-binding site. Mol. Microbiol. 6, 1219–1229.

Sakato, K., Tanaka, H., Shibata, S., Kuratsu, Y., 1992. Agitation-aeration studies on coenzyme Q_{10} production using *Rhodopseudomonas spheroides*. Biotechnol. Appl. Biochem. 16, 19–22.

Sambrook, J., Fritsch, E.F., Maniatis, T., 1989. Molecular Cloning: A Laboratory Manual. Cold Spring Harbor Laboratory Press, New York, NY.

Schmelzer, C., Lindner, I., Vock, C., Fujii, K., Doring, F., 2007. Functional connections and pathways of coenzyme Q_{10}-inducible genes: an in-silico study. IUBMB Life 59, 628–633.

Schmelzer, C., Okun, J.G., Haas, D., Higuchi, K., Sawashita, J., Mori, M., Doring, F., 2010. The reduced form of coenzyme Q_{10} mediates distinct effects on cholesterol metabolism at the transcriptional and metabolite level in SAMP1 mice. IUBMB Life 62, 812–818.

Shults, C.W., Oakes, D., Kieburtz, K., Beal, M.F., Haas, R., Plumb, S., Juncos, J.L., Nutt, J., Shoulson, I., Carter, J., Kompoliti, K., Perlmutter, J.S., Reich, S., Stern, M., Watts, R.L., Kurlan, R., Molho, E., Harrison, M., Lew, M., 2002. Effects of coenzyme Q_{10} in early Parkinson disease: evidence of slowing of the functional decline. Arch. Neurol. 59, 1541–1550.

Singh, R.B., Wander, G.S., Rastogi, A., Shukla, P.K., Mittal, A., Sharma, J.P., Mehrotra, S.K., Kapoor, R., Chopra, R.K., 1998. Randomized, double-blind placebo-controlled trial of coenzyme Q_{10} in patients with acute myocardial infarction. Cardiovasc. Drugs Ther. 12, 347–353.

Suzuki, K., Ueda, M., Yuasa, M., Nakagawa, T., Kawamukai, M., Matsuda, H., 1994. Evidence that *Escherichia coli ubiA* product is a functional homolog of yeast COQ2, and the regulation of *ubiA* gene expression. Biosci. Biotechnol. Biochem. 58, 1814–1819.

Takahashi, S., Nishino, T., Koyama, T., 2003. Isolation and expression of *Paracoccus denitrificans* decaprenyl diphosphate synthase gene for production of ubiquinone-10 in *Escherichia coli*. Biochem. Eng. J. 16, 183–190.

Thomason, L.C., Costantino, N., Court, D.L., 2007. *E. coli* genome manipulation by P1 transduction. Curr. Protoc. Mol. Biol. (Chapter 1, Unit 1.17).

Tran, U.C., Marbois, B., Gin, P., Gulmezian, M., Jonassen, T., Clarke, C.F., 2006. Complementation of *Saccharomyces cerevisiae* coq7 mutants by mitochondrial targeting of the *Escherichia coli* UbiF polypeptide: two functions of yeast Coq7 polypeptide in coenzyme Q biosynthesis. J. Biol. Chem. 281, 16401–16409.

Van Dyk, T.K., Templeton, L.J., Cantera, K.A., Sharpe, P.L., Sariaslani, F.S., 2004. Characterization of the *Escherichia coli* AaeAB efflux pump: a metabolic relief valve? J. Bacteriol. 186, 7196–7204.

Wagner, S., Bader, M.L., Drew, D., de Gier, J.W., 2006. Rationalizing membrane protein overexpression. Trends Biotechnol. 24, 364–371.

Wang, K.C., Ohnuma, S., 2000. Isoprenyl diphosphate synthases. Biochim. Biophys. Acta. 1529, 33–48.

Weaver, L.M., Herrmann, K.M., 1990. Cloning of an *aroF* allele encoding a tyrosine-insensitive 3-deoxy-D-arabino-heptulosonate 7-phosphate synthase. J. Bacteriol. 172, 6581–6584.

Wissenbach, U., Kroger, A., Unden, G., 1990. The specific functions of menaquinone and demethylmenaquinone in anaerobic respiration with fumarate, dimethylsulfoxide, trimethylamine N-oxide and nitrate by *Escherichia coli*. Arch. Microbiol. 154, 60–66.

Wu, Z., Du, G., Chen, J., 2003. Effects of dissolved oxygen concentration and DO-stat feeding strategy on CoQ_{10} production with *Rhizobium radiobacter*. World J. Microbiol. Biotechnol. 19, 925–928.

Yang, X., Dai, G., Li, G., Yang, E.S., 2010. Coenzyme Q_{10} reduces beta-amyloid plaque in an APP/PS1 transgenic mouse model of Alzheimer's disease. J. Mol. Neurosci. 41, 110–113.

Yen, H.W., Feng, C.Y., Kang, J.L., 2010. Cultivation of *Rhodobacter sphaeroides* in the stirred bioreactor with different feeding strategies for CoQ(10) production. Appl. Biochem. Biotechnol. 160, 1441–1449.

Yen, H.W., Shih, T.Y., 2009. Coenzyme Q_{10} production by *Rhodobacter sphaeroides* in stirred tank and in airlift bioreactor. Bioprocess Biosyst. Eng. 32, 711–716.

Yoshida, H., Kotani, Y., Ochiai, K., Araki, K., 1998. Production of ubiquinone-10 using bacteria. J. Gen. Appl. Microbiol. 44, 19–26.

Yoshida, Y., Hayakawa, M., Habuchi, Y., Niki, E., 2006. Evaluation of the dietary effects of coenzyme Q in vivo by the oxidative stress marker, hydroxyoctadecadienoic acid and its stereoisomer ratio. Biochim. Biophys. Acta 1760, 1558–1568.

Young, I.G., Stroobant, P., Macdonald, C.G., Gibson, F., 1973. Pathway for ubiquinone biosynthesis in *Escherichia coli* K-12: gene-enzyme relationships and intermediates. J. Bacteriol. 114, 42–52.

Zahiri, H.S., Noghabi, K.A., Shin, Y.C., 2006a. Biochemical characterization of the decaprenyl diphosphate synthase of *Rhodobacter sphaeroides* for coenzyme Q(10) production. Appl. Microbiol. Biotechnol. 73, 796–806.

Zahiri, H.S., Yoon, S.H., Keasling, J.D., Lee, S.H., Won Kim, S., Yoon, S.C., Shin, Y.C., 2006b. Coenzyme Q_{10} production in recombinant *Escherichia coli* strains engineered with a heterologous decaprenyl diphosphate synthase gene and foreign mevalonate pathway. Metab. Eng. 8, 406–416.

Zhang, D., Shrestha, B., Li, Z., Tan, T., 2007. Ubiquinone-10 production using *Agrobacterium tumefaciens dps* gene in *Escherichia coli* by coexpression system. Mol. Biotechnol. 35, 1–14.

Zhang, D., Shrestha, B., Niu, W., Tian, P., Tan, T., 2006. Phenotypes and fed-batch fermentation of ubiquinone-overproducing fission yeast using ppt1 gene. J. Biotechnol. 128, 120–131.

Zhu, X., Yuasa, M., Okada, K., Suzuki, K., Nakagawa, T., Kawamukai, M., Matsuda, H., 1995. Production of ubiquinone in *Escherichia coli* by expression of various genes responsible for ubiquinone biosynthesis. J. Biosci. Bioeng. 79, 493–495.